Performance Analysis of Dynamic Spectrum Allocation in Multi-Radio Heterogeneous Networks

Yongjae Kim[1], Yonghoon Choi[2], and Youngnam Han[1(✉)]

[1] Department of Electrical Engineering,
Korea Advanced Institute of Science and Technology (KAIST), Daejeon, Korea
{yongjaekim,ynhan}@kaist.ac.kr

[2] Department of Electrical Engineering, Chonnam National University,
Gwangju, Korea
yh.choi@jnu.ac.kr

Abstract. In heterogeneous networks, multi-radio access technologies (RATs) can coexist for a variety of traffic demands and it is called multi-RAT network. Also, cognitive radio enable to use white space of frequency band, and thus spectrum resources can be dynamically allocated. This paper analyzes an effect of multi-radio access (MRA) users, who simultaneously exploit multi-RATs, on network performance where dynamic spectrum allocation (DSA) is performed. Multi-dimensional Erlang loss (MDEL) model, which is based on queueing, is suitable to describe behaviors of single radio access users in multi-RAT networks under the performing DSA. Based on the MDEL model, extended MDEL model is proposed to investigate the effect of MRA users. As MRA users increase, blocking probability, utilization, and expected processing time of a user in the multi-RAT networks deteriorate, since the MRA users require multiple spectrum resources at a time. Numerical results verify the performance degradation resulted from the MRA users under the DSA and FSA scenarios.

Keywords: Dynamic spectrum allocation · Heterogeneous networks · Multi-radio access technology networks · Multi-radio access user

1 Introduction

In heterogeneous networks (HetNets), users who exploit multi-radio access technologies (RATs) become widely common and many wireless applications for multi-RAT have been developed. Hence, spectrum scarcity is one of important issues in HetNets and many researches have been studied the scarcity problem. A large portion of allocated spectrum is used sporadically and the utilization of allocated spectrum has a geographical variation with a high variance in time [1]. Zhao *et al.* [2] show that the depletion of the spectrum is the result of current fixed spectrum allocation (FSA) policy rather than physical scarcity of frequency

D. Noguet et al. (Eds.): CROWNCOM 2016, LNICST 172, pp. 154–165, 2016.
DOI: 10.1007/978-3-319-40352-6_13

bands. For compensation of underutilized spectrum, J. Mitola *et al.* [3] propose a concept of cognitive radio (CR). The CR enables user equipment to dynamically access the spectrum. This is known as dynamic spectrum access.

Dynamic spectrum access is categorized as opportunistic spectrum access model, spectrum sharing model and dynamic exclusive use model [2,4,5]. Liang *et al.* [4] provide an overview on CR networking. They review physical, medium access control and network layer involved in a CR design. Zhang *et al.* [5] focus on spectrum sharing problem in the view point of convex optimization. Moreover, Kliks *et al.* [6] consider flexible pluralistic licensing concept for 5G wireless networks from spectrum sharing point of view. Akyildiz *et al.* [7] classify CR technologies according to different functionalities such as sensing, decision, sharing, and mobility. Dynamic spectrum allocation (DSA) which belongs to the dynamic exclusive use model denotes that spectrum is exclusively distributed by a central entity for spectrum utilization.

DSA has been considered in many researches for spectrum utilization or revenue. Auction or trading methods of spare frequency bands are introduced in [8–10]. Subramanian *et al.* [8] apply a centralized entity called spectrum broker in multi-RAT network based on dynamic auctions. Each base station (BS) bids for channels depending on their demands. Their objective is to maximize the overall revenue subject to interference in the networks. They exploit greedy algorithm for bidding. However, the greedy algorithm is not an optimal solution. Thus binary integer programming is introduced for spectrum allocation [9] to compensate for drawback of the greedy algorithm. They employ an interference graph based on interference constraints. This scheme obtains an optimal set of binary decisions on whether to allocate or not the channels to BSs. The optimal result is found in accordance multiple objectives of maximization of total revenue and spectrum efficiency. Le *et al.* [10] propose a scheme in which the adjacent cells lease the spectrum to each other to maximize the revenue of HetNets. This scheme can maximize profit of operators and solve inter-system interference issue. Game theory, which is an efficient method for resource optimization algorithms, is applied to design a spectrum trading algorithm. Zhang *et al.* [11] investigate joint subchannel and power allocation in cognitive small cell networks. They formulate resource allocation as a cooperative Nash bargaining game, and near optimal solutions are derived by relaxing variables and using Lambert-W function. Nash bargaining resource allocation algorithm is developed and show to converge to a Pareto-optimal equilibrium. In [12], DSA framework for multi-RAT network is proposed. The available frequency band is divided into sharable spectrum blocks. These blocks are heuristically distributed to each RAT according to the amount of traffic load. Choi *et al.* [13] explore the benefit of multiple transmissions by multi-RATs over a single transmission by a single RAT. The optimal solution is founded with respect to band selection and power allocation using a distributed joint allocation algorithm which is proposed for parallel multi-radio access (MRA) scheme to maximize system capacity. In [13], they consider that each RAT, which is based on orthogonal frequency division multiple access (OFDMA), can allocate the scalable spectrum bandwidth size to users. However, the scalable spectrum bandwidth results in high computation complexity to OFDMA systems.

This paper analyzes the effect of MRA and single radio access (SRA) users in multi-RAT networks under the DSA and FSA scenarios. Under the DSA scenario, total spectrum resources can be distributed to each RAT according to traffic loads, whereas the amount of assigned spectrum to each RAT is fixed in the FSA policy. Therefore, the spectrum resources can be more efficiently used in case of DSA. Each RAT is based on OFDMA allocates subchannels to MRA or SRA users. To analyze an effect of MRA users, mathematical models which describe behaviors of MRA users in multi-RAT networks under DSA and FSA are proposed as queueing models. Using the proposed models, blocking probability (BP), utilization, and processing time of a user are evaluated according to the proportion of MRA users.

2 Effect of Multi-Radio Access

This paper considers a region covered by a set of different N BSs, that is, N RATs are in the region [12], and the multi-RATs belong to same or different network operators. This is called multi-RAT network.

Every RAT is assumed to adopt OFDMA and frequency band of each RAT is divided into multiple subchannels. Suppose that the multi-RAT network has C_T subchannels. Based on the FSA policy, the subchannels are evenly distributed among multi-RATs, i.e., C_T/N. On the other hand, subchannels which are in a multi-RAT network can be shared among multi-RATs where DSA is performed. In this case, it is possible that one of RATs uses all C_T subchannels when the RAT has huge traffic loads. The spectrum scarcity problem can be mitigated by performing DSA. The subchannels are assigned to each RAT according to traffic load when DSA is performed.

When an SRA user access to a RAT, the RAT assigns a subchannel to the user, and therefore an SRA user occupies a subchannel at a time. Similarly, when an MRA user access to multi-RAT, each RAT assigns a subchannel. Hence, multiple subchannels are assigned to the MRA user during access to multi-RATs. When a RAT has no remaining subchannel, a user is dropped, and this phenomenon is known as *blocking*.

2.1 Single Radio Access Users in Multi-Radio Access Technology Network

In this subsection, let us consider a case that only SRA users are in a multi-RAT network. An SRA user occupies a subchannel of the RAT which the SRA user accesses. As mentioned above, based on the FSA policy, each RAT has C_T/N subchannels. On the contrary, under DSA, RAT_k user can use RAT_ls subchannel, because subchannels can be shared.

Multi-dimensional Erlang loss (MDEL) model [14] is composed of multiple Erlang loss models ($M/M/c/c$). The multiple Erlang loss models can share their subchannels, therefore total subchannels are shared in the MDEL model. Hence, the multi-RAT network, where DSA is performed, can be modeled as the MDEL model.

The number of subchannels that users occupy is denoted by c_k, where k is index of RAT, $k \in (1, N)$. Then, $\sum_{k=1}^{N} c_k \leq C_T$. When state of MDEL model is defined as the number of users who occupy subchannels in the network, state space is expressed as

$$S = \left\{ \mathbf{c} = (c_1, \cdots, c_N) \middle| \forall c_k \geq 0, \sum_{k=1}^{N} c_k \leq C_T \right\}, \tag{1}$$

where $\mathbf{c} = (c_1, c_2, \cdots, c_N)$ denotes the state and $k \in (1, N)$. The state space is an N-dimensional Euclidean space. Transition rates are as follows:

$$r(\mathbf{c}, \mathbf{c}') = \begin{cases} \lambda_k, & \text{if } \mathbf{c}' = \mathbf{c} + e_k \\ c_k \mu_k, & \text{if } \mathbf{c}' = \mathbf{c} - e_k \end{cases}, \tag{2}$$

where $\mathbf{c}, \mathbf{c}' \in S$, $k \in (1, N)$, and e_k denotes standard basis of N-dimensional Euclidean space. Arrival and departure process assumed Poisson process, and thus λ_k and μ_k are rate values of exponential distribution. In steady-state, balance equation can be derived by using (1) and (2).

$$\begin{aligned} p_{(c_1, \cdots, c_N)} \cdot \sum_{k=1}^{N} \left[I \left(\sum_{i=1}^{N} c_i < C_T \right) \lambda_k + c_k \mu_k \right] \\ = \sum_{k=1}^{N} \left[\lambda_k p_{(c_1, \cdots, c_k+1, \cdots, c_N)} + (c_k + 1) \mu_k p_{(c_1, \cdots, c_k+1, \cdots, c_N)} \right], \end{aligned} \tag{3}$$

where $p_{(c_1, c_2, \cdots, c_N)}$ represents steady-state probability of the state $(c_1, c_2, \cdots, c_N)$ and $I(A)$ denotes the indicator function of event A. Also, if $\mathbf{c} = (c_1, c_2, \cdots, c_N) \notin S$, then $p_{(c_1, c_2, \cdots, c_N)} = 0$. Using (3) and normalization condition $\sum_{\mathbf{c} \in S} p_{(c_1, c_2, \cdots, c_N)} = 1$, the steady-state probabilities are found as follows:

$$\begin{aligned} p_{(0, \cdots, 0)} &= \left[\sum_{c_1=0}^{C_T} \sum_{c_2=0}^{C_T - c_1} \cdots \sum_{c_N=0}^{C_T - \sum_{i=1}^{N-1} c_i} \prod_{k=1}^{N} \frac{{\lambda_k}^{c_k}}{c_k! {\mu_k}^{c_k}} \right]^{-1}, \\ p_{(c_1, \cdots, c_N)} &= \begin{cases} p_{(0, \cdots, 0)} \cdot \prod_{k=1}^{N} \frac{{\lambda_k}^{c_k}}{c_k! {\mu_k}^{c_k}}, & (c_1, \cdots, c_N) \in S \\ 0, & (c_1, \cdots, c_N) \notin S \end{cases}. \end{aligned} \tag{4}$$

2.2 Multi-Radio Access Users in Multi-Radio Access Technology Network

Multi-Radio Access Technology Network with Dynamic Spectrum Allocation: The state space of extended MEDL model is same with the MDEL model.

To describe the behaviors of MRA users in multi-RAT network, the MDEL model is extended. Two state transitions are added to the extended MDEL model. Let $1-\gamma_k$ be the proportion of MRA users, and γ_k be the proportion of SRA users. Then the transition rates are given as follows:

$$r(\mathbf{c},\mathbf{c}') = \begin{cases} \gamma_k\lambda_k, & \text{if } \mathbf{c}' = \mathbf{c} + e_k \\ \gamma_k c_k \mu_k, & \text{if } \mathbf{c}' = \mathbf{c} - e_k \\ \sum\limits_{k=1}^{N} (1-\gamma_k)\lambda_k, & \text{if } \mathbf{c}' = \mathbf{c} + \sum\limits_{k=1}^{N} e_k \\ \sum\limits_{k=1}^{N} (1-\gamma_k)c_k\mu_k, & \text{if } \mathbf{c}' = \mathbf{c} - \sum\limits_{k=1}^{N} e_k \end{cases}, \quad (5)$$

where $\mathbf{c}, \mathbf{c}' \in S$ and $k \in (1, N)$. The third line of (5) denotes that subchannels are assigned to an MRA user. An MRA user simultaneously uses N RATs, and thus N subchannels are assigned. The fourth line of (5) denotes that an MRA user releases assigned subchannel. Figure 1 shows state transitions of multi-RAT network under DSA when MRA users are considered. Using (1) and (5), balance equation is derived in steady-state as (6). Normalization condition and (6), the steady-state probabilities can be computed using numerical approach [15].

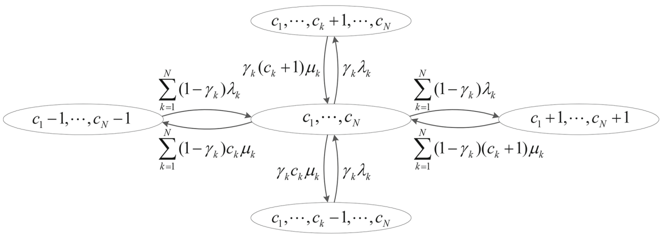

Fig. 1. State transition diagram for behaviors of MRA user in multi-RAT system

$$\begin{aligned} & p_{(c_1,\cdots,c_N)} \Bigg[\sum_{k=1}^{N} I\left((c_1,\cdots,c_k+1,\cdots c_N)\in S\right)\gamma_k\lambda_k + \sum_{k=1}^{N} I\left((c_1,\cdots,c_k-1,\cdots c_N)\in S\right)\gamma_k c_k\mu_k \\ & \quad + \sum_{k=1}^{N} I\left((c_1+1,\cdots c_N+1)\in S\right)(1-\gamma_k)\lambda_k + \sum_{k=1}^{N} I\left((c_1-1,\cdots c_N-1)\in S\right)(1-\gamma_k)c_k\mu_k \Bigg] \\ & = I\left((c_1+1,\cdots c_N+1)\in S\right) p_{(c_1+1,\cdots,c_N+1)} \left(\sum_{k=1}^{N} (1-\gamma_k)(c_k+1)\mu_k \right) \\ & \quad + I\left((c_1-1,\cdots c_N-1)\in S\right) p_{(c_1-1,\cdots,c_N-1)} \left(\sum_{k=1}^{N} (1-\gamma_k)\lambda_k \right) \\ & \quad + \sum_{k=1}^{N} \Big[I\left((c_1,\cdots,c_k-1,\cdots c_N)\in S\right) p_{(c_1,\cdots,c_k-1,\cdots,c_N)}\gamma_k\lambda_k \\ & \quad + I\left((c_1,\cdots,c_k+1,\cdots c_N)\in S\right) p_{(c_1,\cdots,c_k+1,\cdots,c_N)}\gamma_k(c_k+1)\mu_k \Big] \end{aligned} \quad (6)$$

Multi-Radio Access Technology Network with Fixed Spectrum Allocation: Difference between DSA and FSA in the multi-RAT network is whether there are sharable subchannels. Under the FSA policy, every RAT exclusively uses subchannels and there are no sharable subchannels. If there is a gap in the traffic loads among multi-RATs, the FSA is inefficient resources management method compared with DSA.

In case of FSA, the state space is expressed as follows:

$$S = \left\{ \mathbf{c} = (c_1, \cdots, c_N) \middle| 0 \leq c_k \leq \frac{C_T}{N}, \ k \in (1, N) \right\}. \tag{7}$$

Figure 2 shows the difference of state spaces and state transitions between DSA and FSA. In Fig. 2, solid arrows denote the transitions associated with SRA users, whereas dashed arrows denote the transitions associated with MRA users. The state transitions and transition rates are same with DSA as described in (5) and Fig. 1, respectively.

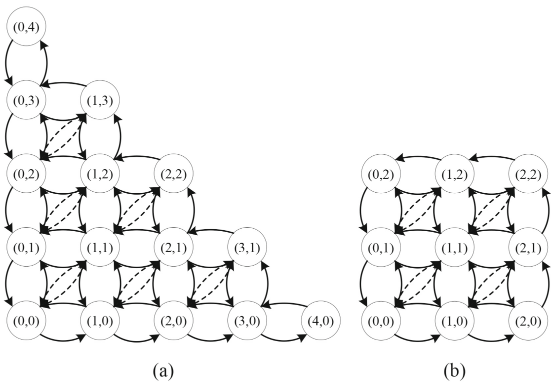

Fig. 2. State transition diagram of extended MDEL model under (a) DSA and (b) FSA, when $C_T = 4$ and $N = 2$

3 Performance Evaluations

3.1 Blocking Probability

Let the probability of the number of total users in the network be π_j, and then it is computed as follows:

$$\pi_j(\boldsymbol{\gamma}, \boldsymbol{\rho}) = \sum_{\mathbf{c} \in S_j} p_{(c_1, \cdots, c_N)}(\boldsymbol{\gamma}, \boldsymbol{\rho}), \tag{8}$$

where $S_j = \left\{ \mathbf{c} = (c_1, \cdots, c_N) \in S \middle| \forall c_k \geq 0, \sum_{k=1}^{N} c_k = j \right\}$, $k \in (1, N)$, $\boldsymbol{\gamma} = (\gamma_1, \cdots, \gamma_N)$, and $\boldsymbol{\rho} = (\rho_1, \cdots, \rho_N) = \left(\frac{\lambda_1}{\mu_1}, \cdots, \frac{\lambda_N}{\mu_N} \right)$. In addition, BP which is defined as a probability that an arrival user is blocked because a RAT has no remaining subchannels is derived by using PASTA theorem, i.e.,

$$BP(\boldsymbol{\gamma}, \boldsymbol{\rho}) = \sum_{\mathbf{c} \in S_B} p_{(c_1, \cdots, c_N)}(\boldsymbol{\gamma}, \boldsymbol{\rho}) = \pi_{C_T}(\boldsymbol{\gamma}, \boldsymbol{\rho}), \tag{9}$$

where $S_B = \left\{ (c_1, \cdots, c_N) \in S \middle| \sum_{k=1}^{N} c_k = C_T \right\}$.

3.2 Utilization

The expected value of the number of total users in the network is given as $L(\boldsymbol{\gamma}, \boldsymbol{\rho}) = \sum_{j=1}^{C_T} j \cdot \pi_j(\boldsymbol{\gamma}, \boldsymbol{\rho})$, and thus utilization is defined as

$$U(\boldsymbol{\gamma}, \boldsymbol{\rho}) = \frac{L(\boldsymbol{\gamma}, \boldsymbol{\rho})}{C_T}. \tag{10}$$

3.3 Processing Time

Assume that a blocked user tries to access a RAT again until the user succeed in accessing the RAT. Using above BPs, processing time $T(\boldsymbol{\gamma}, \boldsymbol{\rho})$ for a user is derived as follows:

$$\begin{aligned} T(\boldsymbol{\gamma}, \boldsymbol{\rho}) =& \Pr[\mathbf{c}^1 \notin S_B] \cdot T_s(\mu) \\ &+ \sum_{n=2}^{\infty} \Pr[\mathbf{c}^2, \cdots, \mathbf{c}^{n-1} \in S_B, \mathbf{c}^n \notin S_B] \cdot (T_s(\mu) + \sum_{m=1}^{n-1} T_i(\lambda)), \end{aligned} \tag{11}$$

where $\mathbf{c}^\tau$ represents the state after τ-th state transition, and random variables T_s and T_i denote service time and inter-arrival time, respectively. $\Pr[\mathbf{c}^1 \notin S_B]$ and $\Pr[\mathbf{c}^2, \cdots, \mathbf{c}^{n-1} \in S_B, \mathbf{c}^n \notin S_B]$ denote the probability that a user is not blocked at the first arrival and the probability that a user in not blocked n-th arrival after $(n-1)$-th blocked. In (11), the probability that user is sequentially blocked is too small, and therefore (11) can be rewritten as follows:

$$T(\boldsymbol{\gamma}, \boldsymbol{\rho}) \cong \Pr[\mathbf{c}^1 \notin S_B] \cdot T_s(\mu) + \Pr[\mathbf{c}^1 \in S_B, \mathbf{c}^2 \notin S_B] \cdot (T_s(\mu) + T_i(\lambda)). \tag{12}$$

The first term of right-hand side in (12) can be rewritten $(1 - BP(\boldsymbol{\gamma}, \boldsymbol{\rho})) \cdot T_s(\mu)$, and then it is also expressed according to which RAT user:

$$\begin{aligned} (1 - BP(\boldsymbol{\gamma}, \boldsymbol{\rho})) \cdot T_s(\mu) &= \sum_{k=1}^{N} Pr[\text{departure user} \in \text{RAT}_k] \cdot (1 - BP(\boldsymbol{\gamma}, \boldsymbol{\rho})) \cdot T_s(\mu_k) \\ &= \sum_{k=1}^{N} \frac{\mu_k}{\sum_{i=1}^{N} \mu_i} \cdot (1 - BP(\boldsymbol{\gamma}, \boldsymbol{\rho})) \cdot T_s(\mu_k). \end{aligned} \tag{13}$$

In addition, $\Pr[\mathbf{c}^1 \in S_B, \mathbf{c}^2 \notin S_B]$ of (12) is expressed as follows:

$$\begin{aligned}\Pr[\mathbf{c}^1 \in S_B,\, \mathbf{c}^2 \notin S_B] &= \Pr[\,\mathbf{c}^2 \notin S_B\,\big|\mathbf{c}^1 \in S_B\,] \cdot Pr[\mathbf{c}^1 \in S_B] \\ &= \Pr[R_s(\mu)\text{ of at least one of } C_T < T_i(\lambda)] \cdot BP(\boldsymbol{\gamma}, \boldsymbol{\rho}) \\ &\overset{(a)}{=} (1 - \Pr[R_s(\mu) > T_i(\lambda)])^{C_T} \cdot BP(\boldsymbol{\gamma}, \boldsymbol{\rho}) \\ &\overset{(b)}{=} (1 - \Pr[T_s(\mu) > T_i(\lambda)])^{C_T} \cdot BP(\boldsymbol{\gamma}, \boldsymbol{\rho}),\end{aligned} \tag{14}$$

where $R_s(\mu)$ represents remaining time of a user. The equality (a) results from the independent-identically distributed (i.i.d.) condition and (b) results from the memoryless property of arrival/departure process. $\Pr[T_s(\mu) > T_i(\lambda)]$ in (14) can be expressed according to which RAT user:

$$\begin{aligned}\Pr[T_s(\mu) > T_i(\lambda)] &= \sum_{k=1}^{N}\sum_{l=1}^{N} \Pr[T_s(\mu_l) > T_i(\lambda_k)] \cdot Pr[\text{arrival user} \in \text{ RAT}_k] \\ &\qquad \cdot \Pr[\text{departure user} \in \text{ RAT}_l] \\ &= \sum_{k=1}^{N}\sum_{l=1}^{N} \frac{\lambda_k}{\lambda_k + \mu_l} \cdot \frac{\lambda_k}{\sum_{i=1}^{N} \lambda_i} \cdot \frac{\mu_l}{\sum_{i=1}^{N} \mu_i}.\end{aligned} \tag{15}$$

After some manipulations, distribution of processing time of a user can be presented as (16) where the number of RATs N is 2. From (16), moment generating function of T is calculated as follows:

$$\begin{aligned}f_T(t) &= \sum_{i=1}^{2}\sum_{j=1}^{2}\left[\beta_{01}\beta_{02}\left(\frac{\alpha_{02}\alpha_{ij}}{\alpha_{ij}\mu_2 - \alpha_{02}\lambda_i}\right)^2 + \sum_{k=0}^{2}\sum_{l=1}^{2}\frac{\alpha_{ij}\alpha_{kl}\omega_{kl}}{\alpha_{ij}\mu_l - \alpha_{kl}\lambda_i}\right]\eta_{ij}e^{-\frac{\lambda_i}{\alpha_{ij}}t} \\ &+ \sum_{i=0}^{2}\sum_{j=1}^{2}\left[\alpha_{ij}\omega_{ij}\left(\sum_{k=1}^{2}\sum_{l=1}^{2}\frac{\alpha_{kl}\eta_{kl}}{\alpha_{ij}\lambda_k - \alpha_{kl}\mu_j}\right)\right. \\ &\left. + I(i=0,\, j=2)\beta_{01}\beta_{02}\left(\sum_{k=1}^{2}\sum_{l=1}^{2}\frac{\alpha_{ij}\alpha_{kl}\eta_{kl}}{\alpha_{ij}\lambda_k - \alpha_{kl}\mu_j}\cdot t - \left(\frac{\alpha_{ij}\alpha_{kl}}{\alpha_{ij}\lambda_k - \alpha_{kl}\mu_j}\right)^2\eta_{kl}\right)\right] e^{-\frac{\mu_j}{\alpha_{ij}}t},\end{aligned} \tag{16}$$

$$\text{where } \alpha_{ij} = \begin{cases} \frac{\mu}{\sum_{k=1}^{2}\mu_k}(1 - BP(\gamma, \rho)), & i = 0 \\ \left[1 - \left(\frac{\lambda_i}{\lambda_i+\mu_j}\cdot\frac{\lambda_i}{\sum_{k=1}^{2}\lambda_k}\cdot\frac{\mu_j}{\sum_{k=1}^{2}\mu_k}\right)^{C_t}\right]\cdot BP(\gamma,\rho), & i \neq 0 \end{cases},$$

$$\beta_{ij} = \frac{\alpha_{ij}\mu_j}{\prod_{k=0,k\neq i}^{2}(\alpha_{ij} - \alpha_{kj})},$$

$$\omega_{ij} = \begin{cases} \left(\frac{\sum_{k=0}^{2}\alpha_{k,j+1}\beta_{k,j+1}}{\mu_j} - \sum_{k=1}^{2}\frac{{\alpha_{k,j+1}}^2\beta_{k,j+1}}{\alpha_{k,j+1}\mu_j - \alpha_{ij}\mu_{j+1}}\right)\frac{\beta_{ij}\mu_j}{\mu_{j+1}}, & i=0, j=1 \\ \sum_{k=1}^{2}\frac{\alpha_{k,j-1}\beta_{k,j-1}}{\alpha_{ij}\mu_{j-1} - \alpha_{k,j-1}\mu_j}, & i=0, j=2 \\ \sum_{k=1}^{2}\frac{\alpha_{k,j+1}\beta_{k,j+1}}{\alpha_{ij}\mu_{j+1} - \alpha_{k,j+1}\mu_j}\alpha_{ij}\beta_{ij}, & i\neq 0, j=1 \\ \sum_{k=1}^{2}\frac{\alpha_{k,j-1}\beta_{k,j-1}}{\alpha_{ij}\mu_{j-1} - \alpha_{k,j-1}\mu_j}\alpha_{ij}\beta_{ij} & i\neq 0, j=2 \end{cases},$$

$$\eta_{ij} = \begin{cases} \frac{(-1)^{j+1}\alpha_{ij}\lambda_i\lambda_{i+1}}{\prod_{m=1}^{2}\left(\sum_{n=1}^{2}(-1)^{n+1}\alpha_{mn}\right)} \sum_{k=1}^{2}(-1)^{k+1}\frac{\alpha_{i+1,k}}{\alpha_{ij}\lambda_{i+1}-\alpha_{i+1,k}\lambda_i}, & i=1 \\ \frac{(-1)^{j+1}\alpha_{ij}\lambda_{i-1}\lambda_i}{\prod_{m=1}^{2}\left(\sum_{n=1}^{2}(-1)^{n+1}\alpha_{mn}\right)} \sum_{k=1}^{2}(-1)^{k+1}\frac{\alpha_{i-1,k}}{\alpha_{ij}\lambda_{i-1}-\alpha_{i-1,k}\lambda_i}, & i=2 \end{cases},$$

$i \in \{0,1,2\}$, $j \in \{1,2\}$.

$$\Phi_T(s) = \prod_{i\in\{1,3,5\}}\left(\frac{\mu_1}{\mu_1-\alpha_i s}\right)\cdot\prod_{j\in\{2,4,6\}}\left(\frac{\mu_2}{\mu_2-\alpha_j s}\right)\cdot \prod_{k\in\{3,4\}}\left(\frac{\lambda_1}{\lambda_1-\alpha_k s}\right)\cdot\prod_{l\in\{5,6\}}\left(\frac{\lambda_2}{\lambda_2-\alpha_l s}\right). \quad (17)$$

Expected processing time is obtained as follows:

$$E[T(\boldsymbol{\gamma},\boldsymbol{\rho})] = \frac{\sum_{i\in\{1,3,5\}}\alpha_i}{\mu_1}+\frac{\sum_{j\in\{2,4,6\}}\alpha_j}{\mu_2}+\frac{\sum_{k\in\{3,4\}}\alpha_k}{\lambda_1}+\frac{\sum_{l\in\{5,6\}}\alpha_l}{\lambda_2}. \quad (18)$$

4 Numerical Results

The objective of numerical analysis is to examine how MRA users affect the performance metrics given in terms of BP, utilization, and expected processing time. For numerical results, the parameter configuration is set as follows: $\lambda_1 = 3$ [users/s], $\lambda_2 = 0.6, 0.8, 1.0$ [users/s], $\mu_1 = 1.5$ [users/s], $\mu_2 = 1$ [users/s], $C_t = 6$, $N = 2$ and $\gamma_1 = \gamma_2 = \gamma$.

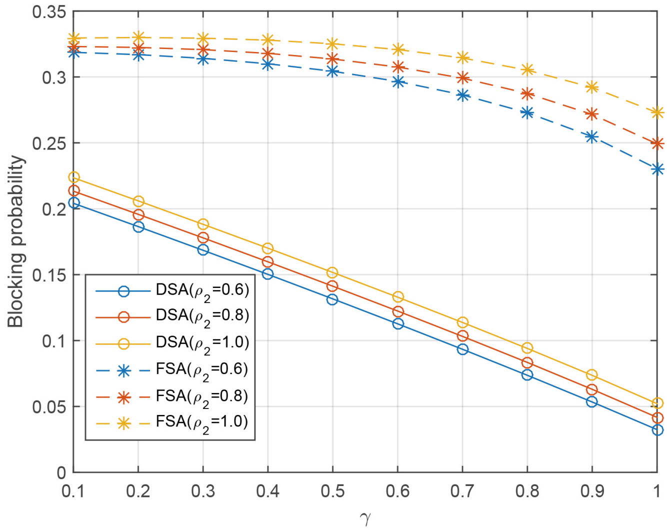

Fig. 3. Blocking probability of DSA and FSA under different γ

Figure 3 presents BPs according to the change in γ under DSA or FSA scenarios. When traffic loads of RAT_2 are low, the BPs are always low in both DSA and FSA cases. If traffic loads are high, the BPs also grow up regardless of which scenario. In addition, BPs always decrease as γ becomes large, because MRA users occupy more subchannels than SRA users at a time. At low γ region, there is no difference of BPs according to γ under FSA, whereas at high γ region, the difference of BPs become large. It describes that DSA is more sensitive with respect to the effects of MRA users than FSA.

Figure 4 shows the utilization of DSA and FSA in accordance with the change in γ. In FSA scenario, the utilization becomes low when MRA users are densely deployed. As γ increases, the utilization also increases. This is because an MRA user need multiple subchannels, whereas an SRA user only needs a subchannel. On the contrary, there is no considerable change according to γ in the utilization of DSA scenario compared to FSA, because DSA takes on a role of load balancing.

Figure 5 illustrates the expected time of processing a user according to different γ under DSA and FSA scenarios. In (18), α_i, $i \in \{3, 4, 5, 6\}$ can be approximated by the terms of $BP(\boldsymbol{\gamma}, \boldsymbol{\rho})$, therefore expected processing time is given by

$$E[T(\boldsymbol{\gamma}, \boldsymbol{\rho})] \cong C_1 \cdot BP(\boldsymbol{\gamma}, \boldsymbol{\rho}) + C_2, \tag{19}$$

where $C_1 = 2\left[\frac{1}{\mu_1+\mu_2}\left(1 + \frac{{\mu_1}^2+{\mu_2}^2}{\mu_1\mu_2}\right) + \frac{\lambda_1+\lambda_2}{\lambda_1\lambda_2}\right]$, and $C_2 = \frac{2}{\mu_1+\mu_2}$. From (19), it is noticed that $E[T(\boldsymbol{\gamma}, \boldsymbol{\rho})] \propto BP(\boldsymbol{\gamma}, \boldsymbol{\rho})$.

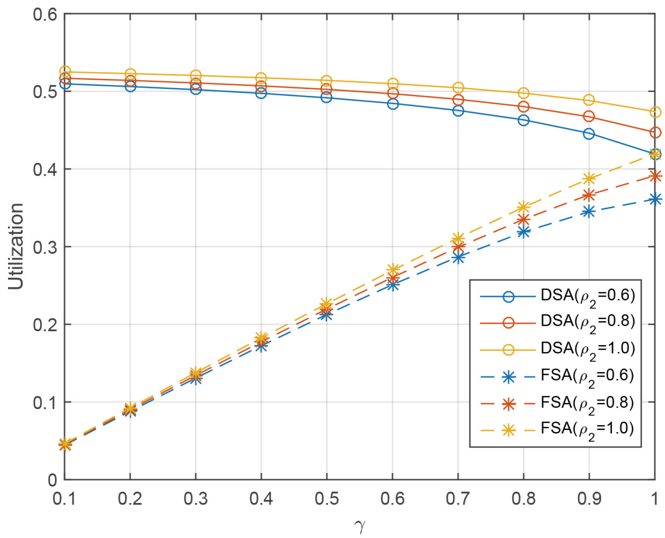

Fig. 4. Utilization of DSA and FSA under different γ

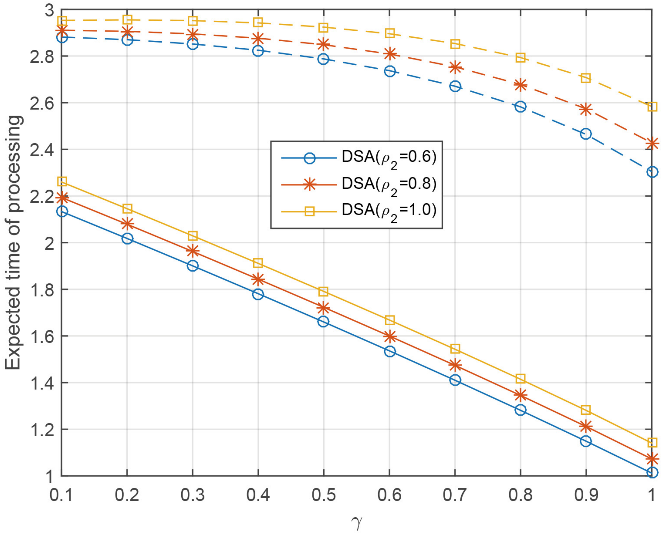

Fig. 5. Expected time of procssing a user under different γ

5 Conclusion

In this paper, an effect of MRA users on performance metrics such as the BP, the utilization, and the expected processing time was analyzed in multi-RAT networks under DSA and FSA scenarios. For this, an analytic model which is extended from MDEL model was provided to describe the behaviors of MRA users. Numerical results verified that DSA gives better performance than FSA and the BP and the expected processing time are improved as the number of SRA users increases.

References

1. Akyildiz, I.F., Lee, W.Y., Vuran, M.C., Mohanty, S.: NeXt generation/dynamic spectrum access/cognitive radio wireless networks: a survey. Comput. Netw. **50**(13), 2127–2159 (2006)
2. Zhao, Q., Sadler, B.M.: A survey of dynamic spectrum access: signal processing, networking, and regulatory policy. IEEE Signal Proc. Mag. **24**(3), 79–89 (2007)
3. Mitola, J., Maguire, G.Q.: Cognitive radio: making software radios more personal. IEEE Pers. Commun. **6**(4), 13–18 (1999)
4. Liang, Y.C., Chen, K.C., Li, G.Y., Mahonen, P.: Cognitive radio networking and communications: an overview. IEEE Trans. Veh. Technol. **60**(7), 3386–3407 (2011)
5. Zhang, R., Liang, Y.C., Cui, S.: Dynamic resource allocation in cognitive radio networks. IEEE Signal Proc. Mag. **27**(3), 102–114 (2010)
6. Kliks, A., Holland, O., Basaure, A., Matinmikko, M.: Spectrum and license flexibility for 5G networks. IEEE Commun. Mag. **53**(7), 42–29 (2015)

7. Akyildiz, I.F., Lee, W.Y., Vuran, M.C., Mohanty, S.: A survey on spectrum management in cognitive radio networks. IEEE Commun. Mag. **46**(4), 40–48 (2008)
8. Subramanian, A.P., Al-Ayyoub, M., Gupta, H., Das, S.R., Buddhikot, M.M.: Near-optimal dynamic spectrum allocation in cellular networks. In: 3rd IEEE Symposium on New Frontiers in Dynamic Spectrum Access networks (DySPAN), pp. 1–11, October 2008
9. Lee, S., Lee, H.: Dynamic spectrum allocation based on binary integer programming under interference graph. In: 23rd International Symposium on Personal Indoor and Mobile Radio Communications (PIMRC), pp. 226–231, September 2012
10. Le, V., Feng, Z., Bourse, D., Zhang, P.: A cell based dynamic spectrum management scheme with interference mitigation for cognitive networks. Wirel. Pers. Commun. **49**(2), 275–293 (2008)
11. Zhang, H., Jiang, C., Beaulieu, N.C., Chu, X., Wang, X., Quek, T.Q.S.: Resource allocation for cognitive small cell networks: a cooperative bargaining game theoretic approach. IEEE Trans. Wireless Commun. **14**(6), 3481–3493 (2015)
12. Alsohaily, A., Sousa, E.S.: Dynamic spectrum management in multi-radio access technology (RAT) cellular systems. IEEE Wirel. Commun. Lett. **3**(3), 249–252 (2014)
13. Choi, Y., Kim, H., Han, S., Han, Y.: Joint resource allocation for parallel multi-radio access in heterogeneous wireless networks. IEEE Trans. Wirel. Commun. **9**(11), 3324–3329 (2010)
14. Melikov, A., Ponomarenko, L.: Multidimensional Queueing Models in Telecommunication Networks. Springer, Heidelberg (2014)
15. Chapra, S.C., Raymond, P.C.: Numerical Methods for Engineers. McGraw-Hill, New York (2012)